Suppression of Stimulated Brillouin Scattering by Increased Landau Damping in Multiple-Ion-Species Hohlraum Plasmas

P. Neumayer, R. L. Berger, L. Divol, D. H. Froula, R. A. London, B. J. MacGowan, N. B. Meezan, J. S. Ross, C. Sorce, L. J. Suter, and S. H. Glenzer

L-399, Lawrence Livermore National Laboratory, P.O. Box 808, Livermore, California 94551, USA

(Received 9 November 2007; published 10 March 2008)

We demonstrate that multiple-ion-species plasmas greatly reduce stimulated Brillouin scattering (SBS) in high-electron temperature inertial confinement fusion hohlraums. Landau damping is increased by adding hydrogen to a CO_2 gas filled hohlraum. We find that the SBS reflectivity decreases monotonically with increasing hydrogen fraction from 18% to 3% with a simultaneous increase of laser beam transmission. Detailed simulations with a 3D laser-plasma interaction code are in agreement with the experimentally observed reduction in backscattered light.

DOI: 10.1103/PhysRevLett.100.105001 PACS numbers: 52.38.Bv, 52.25.Os, 52.35.Fp, 52.50.Jm

In the indirect-drive approach to inertial confinement fusion [1] (ICF) a deuterium-tritium filled fusion capsule is compressed by the ablation pressure from soft x rays inside a laser heated radiation cavity (hohlraum) [2,3]. With the National Ignition Facility (NIF) nearing completion [4], 192 laser beams with a total UV energy of >1 MJ will be available to heat cm-scale hohlraums to radiation temperatures of 270–300 eV [5,6]. To reach these temperatures, the laser beams have to propagate over a length of 3–7 mm through underdense plasma at electron temperatures of $T_e = 2.5$–5 keV before depositing their energy into the hohlraum wall [7]. Stimulated scattering processes in both the high-Z blow-off plasma from the hohlraum wall and the low-Z gas-fill plasma can backscatter the laser light by parametric laser-plasma instabilities, i.e., stimulated Brillouin scattering (SBS) and stimulated Raman scattering (SRS). These processes strongly depend on laser and plasma conditions, which must be tailored to optimize soft x-ray drive and radiation symmetry as required to compress the fusion fuel to ignition conditions.

Recent studies have focused on reducing peak laser beam speckle intensities by employing continuous phase plates (CPP) [8,9] and advanced beam smoothing techniques such as polarization smoothing (PS) and smoothing by spectral dispersion (SSD) [10,11]. These techniques have been shown to improve laser coupling into gas filled hohlraums [12,13] and gas bag targets [14].

An important parameter in controlling laser-plasma interactions is plasma wave damping. Landau damping due to electrons is small and of the order of $\nu_L/\omega_a = 0.01$, due to the large mass difference between electrons and ions. Here ν_L is the damping rate and ω_a is the ion-acoustic frequency. At the high-electron temperatures typical in ICF targets, ion Landau damping in mid- to high-Z single-ion species plasmas is negligible. However, in multiple-ion-species plasmas, the number of particles close to the phase velocity of the SBS-driven ion-acoustic mode is greatly increased, thereby effectively Landau damping the SBS-driven mode [15,16].

A long-standing problem in the field of laser-plasma interactions is a successful demonstration that multiple-ion species plasmas reduce the total backscattering at ICF hohlraum conditions. Although the effect of two-ion species plasmas on Landau damping has been directly observed with Thomson scattering [17], previous laser-plasma interaction experiments have not observed the expected reduction of SBS reflectivity with increased Landau damping [16,18–20]. In addition, the experiments have shown that SRS strongly increased, reaching levels of more than 20% [19]. These experiments have been performed with a limited set of beam smoothing options or in low temperature plasmas where laser beam filamentation exceeds the growth threshold.

In this Letter, we demonstrate for the first time that laser backscattering processes are strongly suppressed in multiple-ion species plasmas that approach ignition hohlraum conditions. Adding hydrogen to a hohlraum filled with CO_2 is shown to reduce the SBS reflected energy of an interaction beam from almost 20% to the percent level. This is accompanied by a simultaneous increase of the transmitted laser light of the interaction beam. In addition, backscatter from the heater beams is strongly suppressed causing an increase in the peak hohlraum radiation temperature due to improved coupling. These experiments were performed in high-electron temperature hohlraums heated with smoothed beams, thus avoiding laser beam filamentation. The measured scaling of SBS is reproduced by linear gain calculations and full-scale 3D laser-plasma interaction calculations. Our findings indicate that SBS can be efficiently controlled by employing multiple-ion species plasmas on future ICF experiments on the NIF.

Figure 1 shows a schematic of the experimental configuration. The experiments were performed at the Omega laser facility at the Laboratory for Laser Energetics (LLE), Rochester [21]. Cylindrically shaped gold hohlraums (2 mm length, 1.6 mm diameter) were filled with ≈1 atm of CO_2. The fill pressure was chosen to yield an electron density of $0.06 n_{\text{crit.}}$, where $n_{\text{crit.}}$ ($\approx 10^{22}$ cm^{-3}) is the criti-

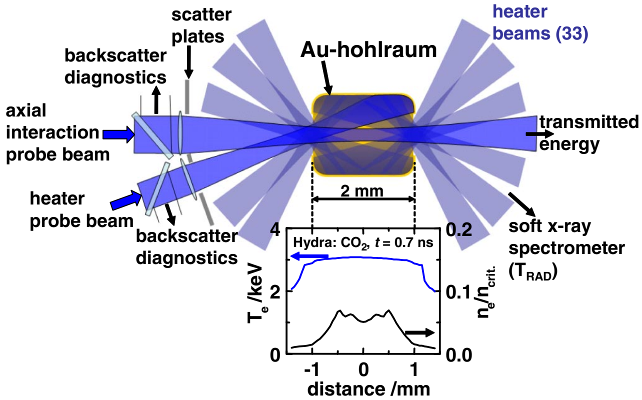

FIG. 1 (color online). Schematic of the experimental setup. The cylindrical hohlraum is heated by 33 heater beams with 14.3 kJ of energy in a 1 ns long square pulse. Radiation-hydrodynamic calculations show electron temperatures of 3 keV. Backscatter diagnostics measure the backscattered light from an on-axis probe beam and one of the heater beams. In addition, the transmitted energy of the on-axis probe beam is measured. An absolutely calibrated soft x-ray spectrometer determines the hohlraum radiation temperature.

cal density for the laser light of wavelength $\lambda = 351$ nm. Varying amounts of hydrogen were added to this gas fill as a light ion species by adding a small amount of up to 13% of propane (C_3H_8) and adjusting the total fill pressure to keep the electron density constant. The short time of 1/2 hour between filling the hohlraums and the experiment ensured that outgassing had a negligible effect on the gas composition.

The hohlraum targets were heated by 33 (351 nm) heater beams in a 1 ns long pulse. The heater beams entered the hohlraum through two circular apertures of 800 μm diameter on either side of the hohlraum. These laser entrance holes were covered with 0.25 μm thick polyimide windows to hold the gas fill. The beams were arranged in 3 cones with entrance angles of approximately 20°, 42°, and 60° to the hohlraum axis. In this study we employed phase plates and polarization smoothing on all beams. The 200 × 300 μm elliptical focal spots were oriented such that the projection onto the laser entrance holes was close to circular. Polarization smoothing using distributed phase rotators was employed to reduce peak intensities from speckles in the focal intensity distribution.

Typical laser energies of 435 J per heater beam result in an intensity of 9×10^{14} W/cm^2 at the hohlraum wall, well below the threshold intensity for ponderomotively driven filamentation $I_{\text{thresh.}} \propto T_e/n_e \approx 1.7 \times 10^{15}$ W/cm^2 for our conditions [22]. This irradiation produced radiation temperatures of 235 eV as measured by an absolutely calibrated soft x-ray spectrometer [23].

The hohlraum target platform has been extensively studied in earlier experiments (see, e.g., [24]). Using Thomson scattering, the electron temperature has been measured to reach peak values of 3.5 keV in good agreement with 2D radiation-hydrodynamic simulations using the code HYDRA [25].

In addition to the heater beams, a laser-plasma interaction probe beam of 351 nm wavelength was propagated along the cylinder axis. A continuous phase plate was used to achieve a focal spot size of 250 μm at the center of the hohlraum. The probe beam was delayed by 0.3 ns with respect to the heater beams. The intensity of the probe beam was varied between 3.6×10^{14} and 1.2×10^{15} W/cm^2 by varying the total energy of the 1 ns long square pulse.

Figure 2 shows time-resolved spectra of SBS backscattered light from the on-axis probe beam. The probe beam intensity for these shots was 3.6×10^{14} W/cm^2. The hydrogen fraction, defined as $r_{\text{H}} := n_{\text{H}}/n_{\text{C,O}}$, where n is the atomic number density, increases from $r_{\text{H}} = 0$, 0.04, 0.08, to 0.35. The data clearly show the reduction in SBS with increasing hydrogen fraction. The total backscattered energy was reduced by more than a factor of 6 from 18% to 2.8%. In addition to the backscattered light, the total trans-

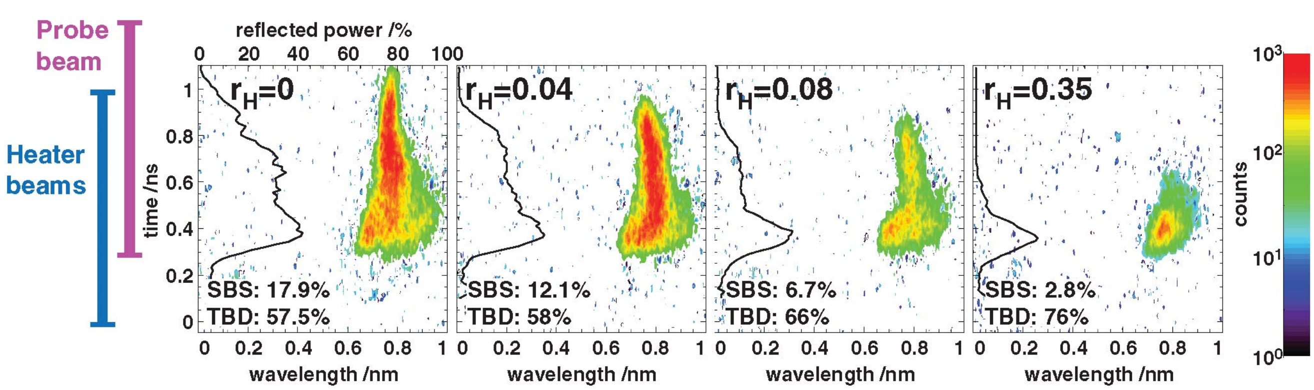

FIG. 2 (color). Streaked spectra of the backscattered light from the on-axis interaction probe beam. The hydrogen fraction r_H and the backscattered and transmitted energies are denoted in the images. The probe beam intensity in these shots was $I = 3.6 \times 10^{14}$ W/cm^2. The images are corrected for differences in neutral-density filtering from shot to shot. The lineouts show the fraction of scattered SBS power, according to the upper axis.

mitted energy of the on-axis probe beam was measured. With decreasing backscatter the transmitted energy increased by approximately the same amount such that the sum of backscattered and transmitted beam energy remained roughly constant at 70%–80%.

The backscattered light from the on-axis probe beam and from one of the heater beams was measured by a comprehensive suite of backscatter diagnostics. Light that is backscattered into the final focusing lens aperture is down-collimated and time-resolved spectra are recorded by two streaked spectrometers covering the wavelength range of (351 ± 3) nm for SBS and 450–700 nm for SRS. The total backscattered energy in either of these spectral ranges is measured by calorimeters. The energy response was calibrated by propagating a laser pulse of known energy from the target chamber center directly into the instrument. We estimate the absolute measurement uncertainty of the backscattered energy to $\pm 10\%$.

Backscattered light outside the final focusing lens aperture is diffusely scattered from Spectralon (R) (Labsphere, Inc.) coated aluminum plates surrounding the lens apertures. The scatter plates are imaged onto two CCD cameras, spectrally filtered for the SBS and SRS wavelength range. The energy response of this system was calibrated in both wavelength regimes by locally illuminating the scatter plates with individual laser pulses of known energy at wavelengths of 355 and 532 nm. The total near-backscattered energy on the scatter plate is determined from the CCD image with an uncertainty of $\pm 10\%$. The energy of the backscattered light measured outside the final focusing lens aperture was small—of the order of a few percent of the energy measured inside the aperture, which is consistent with filamentation being negligible in these experiments.

The spectra in Fig. 2 show a spectrally narrow feature red-shifted by ≈ 0.8 nm from the incident laser wavelength, indicating that SBS is driven in the bulk of the plasma at temperatures of ≈ 3 keV. The reflectivity ceases at $t \approx 1$ ns although the probe pulse extends up to $t = 1.3$ ns, due to a rapid rise of the ion temperature when the shock wave driven by the hohlraum wall blow-off reaches the axis [24].

The time history of the SBS reflected power shows that adding hydrogen to the gas fill reduces the reflected power throughout the entire duration of the pulse. However, while at later times (>0.5 ns) the effect of the increased Landau damping is strong, at early times (0.3–0.5 ns) the reflectivity is less affected. At this early time the electron temperature is below 2 keV and the SBS instability is strongly driven.

Figure 3 shows the instantaneous SBS reflectivity at $t = 0.7$ ns. At this time the plasma electron temperature has increased to $T_e = 3$ keV ($T_i \approx 400$ eV) [24] so the plasma is in the high-electron temperature regime approaching ICF conditions where Landau damping is important in

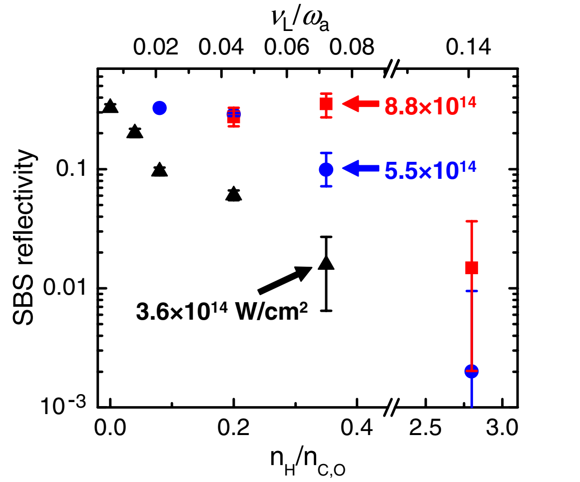

FIG. 3 (color online). Instantaneous SBS reflectivities at $t = 0.7$ ns for interaction beam intensities of 3.6, 5.5 and 8.8×10^{14} W/cm^2. Also shown (upper axis) are the Landau damping values increasing from 0.006 to 0.14.

controlling SBS. For the probe beam intensity of 3.6×10^{14} W/cm^2 the reflected power is gradually reduced from 30% to <2% when increasing the hydrogen fraction to $r_H = 0.35$. This composition change corresponds to a change in Landau damping from $\nu_L/\omega_a = 0.006$ to $\nu_L/\omega_a = 0.072$. For higher probe beam intensities the reflectivity is reduced if higher hydrogen fractions are employed, indicating strong saturation of the SBS instability, e.g., by pump depletion. The error bars are mainly due to the uncertainty in the relative timing of about 100 ps. We note that in all cases the level of SRS backscattered light was below the instrumental detection threshold of $\approx 10^{-4}$.

The reduction of SBS reflectivity with increasing Landau damping is reproduced by linear gain calculations. For the experimental conditions (laser light distribution inside the hohlraum and gas fill), electron and ion temperatures, densities and flow velocities are obtained from radiation-hydrodynamic simulations using HYDRA with an electron flux limiter of 0.1. The plasma parameters are subsequently post-processed with the Laser Interaction Post-Processor (LIP) [26] to calculate temporally and spectrally resolved linear gains for SBS along the path of the probe beam.

Figure 4 shows the scaling of the SBS reflectivity at $t = 0.7$ ns as a function of the calculated linear gain values. The fit to the data was obtained by applying linear theory including pump depletion [27],

$$R(1 - R) = \epsilon \exp \alpha G(1 - R), \qquad (1)$$

where $\epsilon \approx 10^{-9}$ is the thermal noise. Gains obtained by LIP include detuning of the SBS resonance due to axial flow gradients, which becomes increasingly important at smaller damping, i.e., with decreasing resonance width. Therefore, using $G \propto 1/\nu_L$ in Eq. (1) strongly overesti-

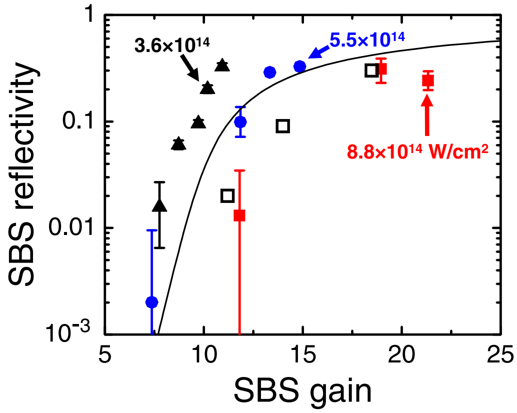

FIG. 4 (color online). Scaling of instantaneous SBS reflectivity with linear gain as the ion acoustic wave Landau damping is varied. The data are fitted using 1D linear theory with pump depletion and a gain multiplier of $\alpha = 1.8$ (solid line). Simulated reflectivities using the code PF3D are shown for $r_H = 0.35$ (open squares).

mates the reflectivities. The gain multiplier $\alpha = 1.8$ was used to account for the effect of speckles, which play an important role in triggering SBS and are not included in this 1D linear gain model. Also shown in Fig. 4 are results from the 3D laser-plasma interaction code PF3D [28]. This code uses realistic beams including micrometer-scale speckles and allows a quantitative prediction of SBS reflectivities. Although the threshold for the onset of SBS is overestimated the simulations reproduce the effect of SBS being reduced by increased Landau damping while maintaining low SRS reflectivities.

Multiple-ion species also have an effect on the hohlraum energetics. As the hydrogen fraction was raised, the hohlraum radiation temperature was measured to increase from 231 to 235 eV. Backscatter measurements on one of the heater beams of the 20° cone show that this increase can be attributed to an improved laser coupling efficiency as the total backscatter from the heater beams is suppressed.

With increasing hydrogen fraction the SBS backscatter on the heater beam was reduced from almost 30% to 8%. The SRS channel shows a small amount (1%–3%) of backscatter. Backscatter from heater beams of the outer cones was accounted for based on results from previous experiments [29]. The total backscattered heater energy is reduced by $\approx 8\%$ when increasing r_H. Using the Marshak scaling of the peak radiation temperature T_{RAD} [30,31] the observed $\Delta T_{\mathrm{RAD}} = 4$ eV corresponds to an increase in heater energy of 7%, which is in good agreement with the observed change in backscatter.

In summary, we have shown that increasing ion Landau damping in high-electron temperature multiple-ion species plasmas strongly suppresses SBS. By adding a low-mass ion species (hydrogen) to a CO_2 hohlraum gas fill, the SBS reflected power was reduced from >30% to below 1%. The reduction in the total backscattered energy leads to an increased laser beam transmission. Furthermore, the suppression of laser backscatter results in an increase of the hohlraum radiation temperature indicating improved coupling of the heater beams. These observations have motivated the use of multiple-ion species plasmas for future indirect-drive ignition experiments on the NIF. The latest ignition hohlraum design features a helium-hydrogen hohlraum gas fill and gold-boron hohlraum wall liner for which PF3D simulations indicate that SBS will be suppressed to negligible values.

This work performed under the auspices of the U. S. Department of Energy by Lawrence Livermore National Laboratory under Contract No. DE-AC52-07NA27344.

[1] J. D. Lindl *et al.*, Phys. Plasmas **11**, 339 (2004).
[2] W. J. Krauser *et al.*, Phys. Plasmas **3**, 2084 (1996).
[3] S. W. Haan *et al.*, Phys. Plasmas **2**, 2480 (1995).
[4] E. I. Moses and C. R. Wuest, Fusion Sci. Technol. **47**, 314 (2005).
[5] S. Atzeni and J. Meyer-ter-Vehn, *The Physics of Inertial Fusion: Beam Plasma Interaction, Hydrodynamics, Hot Dense Matter* (Oxford University, New York, 2004).
[6] L. J. Suter *et al.*, Phys. Plasmas **3**, 2057 (1996).
[7] S. H. Glenzer *et al.*, Nature Phys. **3**, 716 (2007).
[8] Y. Kato *et al.*, Phys. Rev. Lett. **53**, 1057 (1984).
[9] R. L. Kauffman *et al.*, Phys. Plasmas **5**, 1927 (1998).
[10] K. Tsubakimoto *et al.*, Opt. Commun. **91**, 9 (1992).
[11] S. Skupsky *et al.*, J. Appl. Phys. **66**, 3456 (1989).
[12] S. H. Glenzer *et al.*, Phys. Rev. Lett. **80**, 2845 (1998).
[13] C. Niemann *et al.*, Phys. Rev. Lett. **94**, 085005 (2005).
[14] B. J. MacGowan *et al.*, Phys. Plasmas **3**, 2029 (1996).
[15] E. A. Williams *et al.*, Phys. Plasmas **2**, 129 (1995).
[16] D. H. Froula *et al.*, Phys. Rev. Lett. **88**, 105003 (2002).
[17] S. H. Glenzer *et al.*, Phys. Rev. Lett. **77**, 1496 (1996).
[18] R. K. Kirkwood *et al.*, Phys. Rev. Lett. **77**, 2706 (1996).
[19] J. C. Fernández *et al.*, Phys. Plasmas **4**, 1849 (1997).
[20] R. K. Kirkwood *et al.*, Phys. Plasmas **4**, 1800 (1997).
[21] J. M. Soures *et al.*, Phys. Plasmas **3**, 2108 (1996).
[22] E. A. Williams *et al.* Phys. Plasmas **13**, 056310 (2006).
[23] C. Sorce *et al.*, Rev. Sci. Instrum. **77**, 10E518 (2006).
[24] D. H. Froula *et al.*, Phys. Plasmas **13**, 052704 (2006).
[25] M. M. Marinak *et al.*, Phys. Plasmas **8**, 2275 (2001).
[26] N. Meezan *et al.*, Phys. Plasmas **14**, 056304 (2007); L. V. Powers *et al.*, Phys. Plasmas **2**, 2473 (1995).
[27] C. Tang, J. Appl. Phys. **37**, 2945 (1966).
[28] R. L. Berger *et al.*, Phys. Plasmas **5**, 4337 (1998).
[29] S. Regan *et al.*, Bull. Am. Phys. Soc. **52**, NO6.00004 (2007).
[30] R. E. Marshak, Phys. Fluids **1**, 24 (1958).
[31] R. Sigel *et al.*, Phys. Rev. A **38**, 5779 (1988).